

Characterization and Photophysical Properties of Natural Anthraquinone Dyes in Borneo Traditional Pua Kumbu Textile

Nabila Elyana Adnan, Nur Atiqah Mohd Nasuha, Hairul Anuar Tajuddin,
Zanariah Abdullah and Yeun-Mun Choo*

Department of Chemistry, Faculty of Science, University of Malaya, 50603 Kuala Lumpur, Malaysia

*Correspondence author (e-mail: ymchoo@um.edu.my)

Anthraquinone is a natural dye with many applications. The present findings provide valuable information on the photophysical properties of natural anthraquinone, which are previously inaccessible due to unavailability/difficulty in obtaining pure samples. The absorption/emission bands were found to have shifted to the visible region, as a result of hyper-conjugation phenomenon due to the formation of additional quasi aromatic rings between the strategically located substitution groups with the anthraquinone core structure. The formation of the quasi aromatic rings was supported by the observation in the NMR spectra. The results suggested the role of the substitution group in controlling absorption/emission band transitions and selectivity, highlighting anthraquinone potential in the dye and sensor applications.

Key words: Anthraquinone; photophysical property; absorption spectroscopy; emission spectroscopy; NMR spectroscopy; Pua Kumbu

Received: December 2019; Accepted: June 2020

Anthraquinone is one of the most important group of pigments providing a wide range of shades and hues, from red to blue [1]. The color of anthraquinone is determined by the type and position of the substitution group. The structure of anthraquinone is characterized by the presence of the unique anthracene-9,10-dione core structure, and can be obtained from natural sources and chemical syntheses. The position of the substitution group in synthetic anthraquinone is often limited to position-1, -2, -4, and -5 due to synthetic constraint [2,5]. In contrast, natural anthraquinone is found to be more diverse in the position of the substitution group, such as the synthetically less-preferred position-3. Although over 700 natural anthraquinones have been reported [6], the main focus of these reports centered around the chemical

structures and biological activities. The photochemical study on natural anthraquinone has not been given its due attention despite its wide application as natural dye [7-10]. The difficulty in accessing natural anthraquinone samples is one of the major reasons for the limited photophysical report when compared to synthetic anthraquinone.

Natural anthraquinone is an important dye for the traditional dyeing culture in Malaysia. The common source of natural anthraquinone dye in Malaysia is from the roots of *Morinda citrifolia*. It provides yellow-orange color to the Borneo traditional Pua Kumbu textile [11]. We have previously reported the photochemical study on five natural anthraquinones, i.e., nordamnacanthal (**1**), damnacanthal

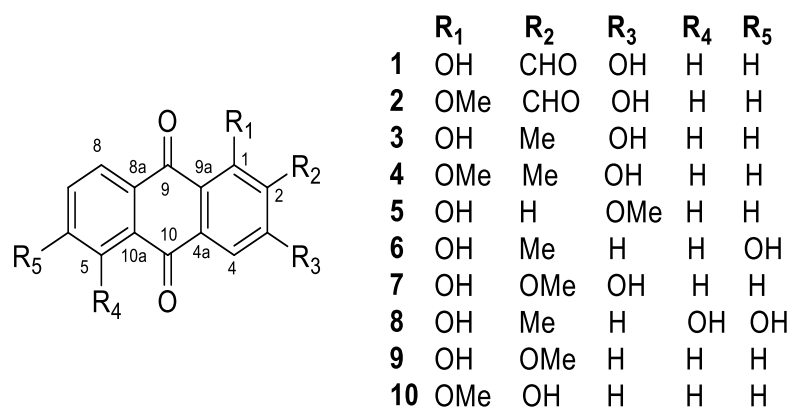


Figure 1. Structures of anthraquinones 1-10

(2), rubiadin (3), 1-methoxy-2-methyl-3-hydroxy-anthraquinone (4), and 1-hydroxy-3-methoxyanthraquinone (5) high-lighting the effect of the substitution group on the absorption and emission spectra [12]. In continuation of our study on natural anthraquinone, we wish to report the characterization and photophysical properties of another five natural anthraquinones, i.e., 1,6-dihydroxy-2-methyl anthraquinone (6), 1,3-dihydroxy-2-methoxy anthraquinone (7), 1,5,6-trihydroxy-2-methyl anthraquinone (8), 1-hydroxy-2-methoxy anthraquinone (9), and 1-methoxy-2-hydroxy anthraquinone (10) from the roots of *Morinda citrifolia* (Fig. 1).

MATERIALS AND METHODS

1. General Experimental Procedures

NMR spectra data were obtained from 600 MHz Bruker AVANCE III (Bruker, Fallanden, Switzerland) with chemical shifts (δ) expressed in ppm and TMS as an internal standard in CDCl_3 or CD_3OD . On the other hand, coupling constants (J) are reported in Hz. Furthermore, ESIMS data were obtained from Agilent 6490 QQQ (Agilent Technologies, Santa Clara, CA, USA) mass-spectrometer equipped with Agilent 1290 series Rapid Resolution LC system (Agilent Technologies, Santa Clara, CA, USA). UV measurement was carried out using Agilent Cary 60 UV-Vis spectrophotometer (Agilent Technologies, Santa Clara, CA, USA). Fluorescence measurement was conducted using Horiba Scientific FluoroMax-4 spectrofluorometer (HORIBA Instruments Incorporated, Edison, NJ, USA). IR measurement was performed on Perkin-Elmer RX1 FT-IR (Perkin Elmer, Waltham, MA, USA) spectrophotometer using NaCl cell.

2. UV and Fluorescence Measurement

Absorption spectra were recorded between 190 and 1100 nm on Cary 60 UV-Vis spectrometer using methanol as the solvent. Emission spectra on the other hand were obtained from Horiba Scientific FluoroMax-4 spectrofluorometer at 25°C and 5 nm slit width for both excitation and emission measurements. Anthraquinone concentrations between 1.42×10^{-4} and 1.57×10^{-4} M were used in the experiments.

3. Extraction and Isolation

The roots of *M. citrifolia* were collected in Kuala Lipis, Pahang, Malaysia. The roots were cut and crushed to smaller pieces before air dried. 0.85 kg of *M. citrifolia* roots was extracted with chloroform and followed by denatured ethanol. Extracts were then concentrated to dryness under reduced pressure to give 8.6 g and 15.4 g of crude chloroform and ethanol extracts, respectively. Crude chloroform extracts were subjected to extensive chromatographic separations to produce the anthraquinones.

2.8 g of the chloroform extract was purified using column chromatography using silica gel 60 (0.040-0.063, Merck, Darmstadt, Germany) and solvent system of chloroform which resulted in 7 fractions (A, B, C, D, E, F, and G). Centrifugal chromatography (Kieselgel 60 with gypsum silica gel; Merck, Darmstadt, Germany) was extensively used for the subsequent isolation and purification of pure compounds. Extensive purification of fraction C using centrifugal chromatography with solvent system chloroform:hexane (6:4) afforded four fractions, C1, C2, C3, and C4. Refractionation of fraction C1 using centrifugal chromatography with solvent system chloroform:hexane (6:4) afforded compounds 10 and 9. While purification of fraction C3 using centrifugal chromatography with solvent system chloroform:hexane (1:1) afforded compound 6, and purification of fraction C4 using centrifugal chromatography with solvent system chloroform:hexane (1:1) afforded compound 7. Purification of fraction G using centrifugal chromatography with solvent system chloroform (100%) afforded compound 8. The yields of the compounds were as follows: 6 (2.6 mg), 7 (2.6 mg), 8 (3.0 mg), 9 (0.9 mg), and 10 (0.8 mg). The isolation method and yields for anthraquinone 1-5 have been described previously [12].

4. 1,6-Dihydroxy-2-methylanthraquinone (6)

Yellow-orange amorphous powder. ESI-MS m/z 253.0 [M-H]⁻ (calculated for $\text{C}_{15}\text{H}_{10}\text{O}_4\text{-H}$, 253.1). ¹H-NMR (CDCl_3 , 600 MHz) δ 13.12 (1H, s, 1-OH), 8.13 (1H, d, $J = 8$, H-8), 7.63 (1H, d, $J = 8$, H-4), 7.50 (1H, s, H-5), 7.43 (1H, d, $J = 8$, H-3), 7.12 (1H, d, $J = 8$, H-7), 2.30 (1H, s, 2-Me). ¹³C-NMR (CDCl_3 , 150 MHz) δ 188.3 (C, C-9), 183.5 (C, C-C-10), 163.7 (C, C-6), 160.9 (C, C-1), 136.7 (CH, C-3), 136.1 (C, C-10a), 135.4 (C, C-2), 131.7 (C, C-4a), 130.1 (CH, C-8), 125.8 (C, C-8a), 121.7 (CH, C-7), 119.3 (CH, C-4), 115.4 (C, C-9a), 113.1 (CH, C-5), 16.4 (C, 2-Me).

5. 1,3-Dihydroxy-2-methoxyanthraquinone (7)

Yellow amorphous powder. ESI-MS m/z 269.0 [M-H]⁻ (calculated for $\text{C}_{15}\text{H}_{10}\text{O}_5\text{-H}$, 269.0). ¹H-NMR (CDCl_3 , 600 MHz) δ 14.81 (1H, s, 1-OH), 12.63 (1H, s, 3-OH), 8.34 (1H, dd, $J = 8$ and 1 Hz, H-8), 8.28 (1H, dd, $J = 8$ and 1 Hz, H-5), 7.82 (1H, m, H-6), 7.82 (1H, m, H-7), 7.40 (1H, s, H-4), 4.08 (1H, s, 2-OMe). ¹³C-NMR (CDCl_3 , 150 MHz) δ 187.8 (C, C-9), 183.0 (C, C-10), 172.1 (C, C-2), 171.2 (C, C-3), 168.5 (C, C-1), 135.0 (CH, C-7), 134.7 (CH, C-6), 133.5 (C, C-8a), 133.5 (C, C-10a), 127.8 (CH, C-5), 127.4 (CH, C-8), 110.0 (C, C-9a), 109.6 (CH, C-4), 106.4 (C, C-4a), 53.4 (C, 2-OMe).

6. 1,5,6-Trihydroxy-2-methylanthraquinone (8)

Orange-red amorphous powder. ESI-MS m/z 269.0 [M-H]⁻ (calculated for $\text{C}_{15}\text{H}_{10}\text{O}_5\text{-H}$, 269.0). ¹H-NMR (CDCl_3 , 600 MHz) δ 7.75 (1H, d, $J = 8$, H-8), 7.68

(1H, d, J = 8, H-4), 7.45 (1H, d, J = 8, H-3), 7.13 (1H, d, J = 8, H-7), 2.32 (1H, s, 2-Me). ¹³C-NMR (CDCl₃, 150 MHz) δ 188.8 (C, C-10), 187.7 (C, C-9), 161.2 (C, C-1), 152.8 (C, C-6), 150.6 (CH, C-5), 136.8 (CH, C-3), 136.1 (C, C-2), 131.4 (C, C-4a), 124.7 (C, C-8a), 121.7 (CH, C-8), 120.6 (CH, C-7), 119.1 (CH, C-4), 116.7 (CH, C-10a), 115.6 (C, C-9a), 16.4 (C, 2-Me).

7. 1-Hydroxy-2-methoxyanthraquinone (9)

Yellow amorphous powder. ESI-MS m/z 253.0 [M-H]⁻ (calculated for C₁₅H₁₀O₅-H, 253.1). ¹H-NMR (CDCl₃, 600 MHz) δ 13.03 (1H, s, 1-OH), 8.32 (1H, m, H-5), 8.32 (1H, m, H-8), 7.86 (1H, m, H-4), 7.82 (1H, m, H-6), 7.82 (1H, m, H-7), 7.79 (1H, d, J = 8, H-3), 4.86 (1H, s, 2-OMe). ¹³C-NMR (CDCl₃, 150 MHz) δ 182.0 (C, C-10), 160.0 (C, C-1), 160.0 (C, C-2), 135.0 (CH, C-3), 135.0 (CH, C-8a), 134.5 (CH, C-6), 134.5 (CH, C-7), 133.7 (C, C-4a), 133.7 (C, C-10a), 127.8 (CH, C-8), 127.3 (CH, C-5), 119.8 (CH, C-4), 115.2 (C, C-9a), 61.0 (C, 2-OMe).

8. 1-Methoxy-2-hydroxyanthraquinone (10)

Yellow amorphous powder. ESI-MS m/z 253.0 [M-H]⁻ (calculated for C₁₅H₁₀O₄-H, 253.1). ¹H-NMR (CDCl₃, 600 MHz) δ 13.02 (1H, s, 2-OH), 8.27 (1H, m, H-5), 8.27 (1H, m, H-8), 8.14 (1H, d, J = 9, H-4), 7.78 (1H, m, H-6), 7.78 (1H, m, H-7), 7.36 (1H, d, J = 9, H-3), 4.04 (1H, s, 1-OMe). ¹³C-NMR (CDCl₃, 150 MHz) δ 181.7 (C, C-10), 155.3 (C, C-2), 146.2 (C, C-1), 134.2 (CH, C-6), 134.2 (CH, C-7), 134.2 (CH, C-8a), 134.2 (C, C-10a), 127.4 (CH, C-4a), 127.1 (C, C-8), 127.1 (CH, C-5), 126.1 (CH, C-4), 126.1 (C, C-9a), 120.6 (CH, C-3), 62.6 (C, 1-OMe).

RESULTS

We have previously reported the photophysical properties for five natural anthraquinones (1-5), possessing mixed electron-withdrawing and -donating

substitution groups at different positions [12]. Despite the presence of the electron-withdrawing and blue-shift promoting CHO substitution group in nordamnacanthal (1), the ability of the 2-CHO group to form an additional quasi aromatic ring with the proximate 3-OH group has resulted in a significant red-shift in both the absorption and emission spectra, demonstrating anthraquinone tuning flexibility from blue- to red-shift. The present report focuses on the photophysical properties of another five natural anthraquinones which possessed primarily electron-donating substitution groups.

1. Absorption Spectra

The absorption spectra of anthraquinones 6-10 displayed bands typical of the anthraquinone chromophore with strong and sharp bands observed at 200-300 nm, and weaker and broader bands at 350-450 nm (Fig. 2 and Table 1) [12-17]. The bands in the blue-shift region were due to the $\pi \rightarrow \pi^*$ transition from the fused aromatic rings and quinone core structure, while the red-shift region bands were due to the $n \rightarrow \pi^*$ transition [12-17]. The absorption bands of anthraquinones 6-10 displayed a general red-shift displacement to the visible region, when compared to anthraquinones 1-5 [12], which was due to the predominant presence of the electron-donating substitutions. The observed absorption bands in 6-10 were also sharper with larger molecular coefficients. The positions of the substitution groups in 6-10 contributed to this observation in two ways. The presence of the electron-donating substitution groups such as OH, OMe, and Me groups in 6-10 resulted the red-shift displacement in the absorption spectra and the effect from the formation of additional quasi aromatic rings through intramolecular bonding. 1,5,6-trihydroxy-substituted anthraquinone 8 displayed the longest visible wavelength maxima at 447 nm, while the highest maxima were displayed by 1,6-dihydroxy-substituted anthraquinone 6 at 411 nm.

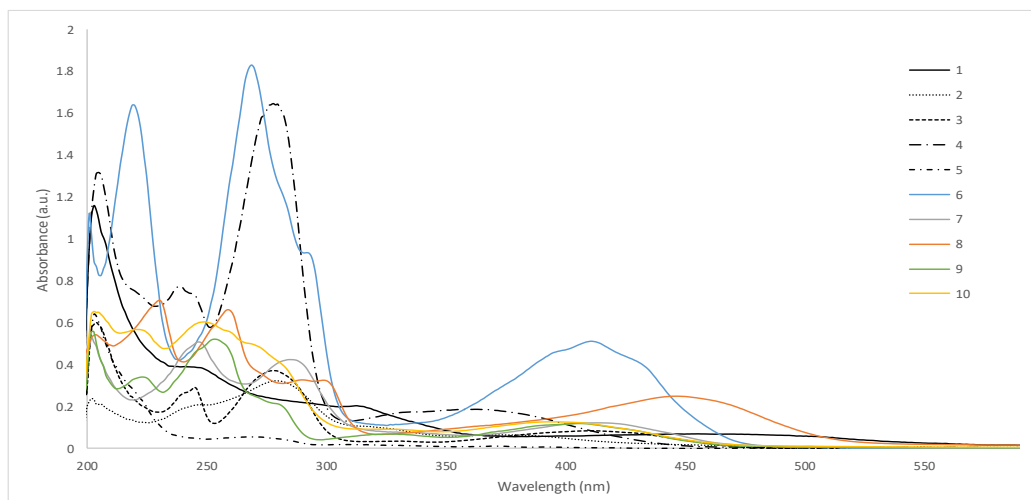


Figure 2. UV-visible absorption of anthraquinones 1-10

Table 1. Absorbance and coefficients of anthraquinones 6-10

Compound	λ_{max} (nm)	Intensity (a.u.)	ϵ (Mcm ⁻¹)
6	201	0.53	3740.23
	219	0.78	5478.41
	269	0.87	6122.07
	411	0.24	1705.99
7	202	0.51	3572.72
	247	0.49	3439.18
	285	0.41	2869.54
	415	0.12	827.06
8	204	0.58	4073.51
	230	0.75	5305.61
	259	0.71	4975.78
	290	0.35	2446.88
	447	0.26	1863.47
9	202	0.53	3723.99
	223	0.32	2274.25
	253	0.49	3485.15
	327	0.06	447.99
	406	0.11	783.95
10	203	0.65	4609.65
	222	0.57	4004.38
	249	0.60	4261.28
	394	0.13	890.34

2. Emission Spectra

The maxima wavelength obtained from the absorption study was excited to obtain the fluorescence spectra (Fig. 3). Anthraquinones **6-10** showed emission bands in the 500-700 nm visible region, while only anthraquinones **8-10** showed additional emission bands in the 300-500 nm region. The emission bands of **6-10** in the 500-700 nm region displayed significant hyperchromic shift when compared to those of **1-5**. The emission maxima, intensity, and Stokes shift values of **6-10** are summarized in Table 2. Anthraquinones **6** and **7** displayed the longest emission maxima with largest Stokes shift at 585 (Stokes shift 316 nm) and 567 (Stokes shift 282 nm) nm, respectively. While the emission maxima for anthraquinones **8-10** were observed at much shorter

wavelengths at around 338-342 nm. In addition, emission bands were also observed in the visible range at a lower intensity in **8-10**.

3. ¹H & ¹³C-NMR Spectra

The anthraquinones displayed highly characteristic NMR spectra. The low field ¹H-NMR signals were associated with the aromatic protons of the anthraquinone core structure. The anisotropic deshielding effect of the C-9 or C-10 carbonyl on the ¹H-protons, such as H-1, H-4, H-5, and H-8, resulted in the low field shift of the signal in the ¹H-NMR spectra. On the other hand, common substitution groups, such as OMe and Me, displayed sharp signals in the high field region in the ¹H-NMR spectra. The observation of the sharp signal for the hydroxyl

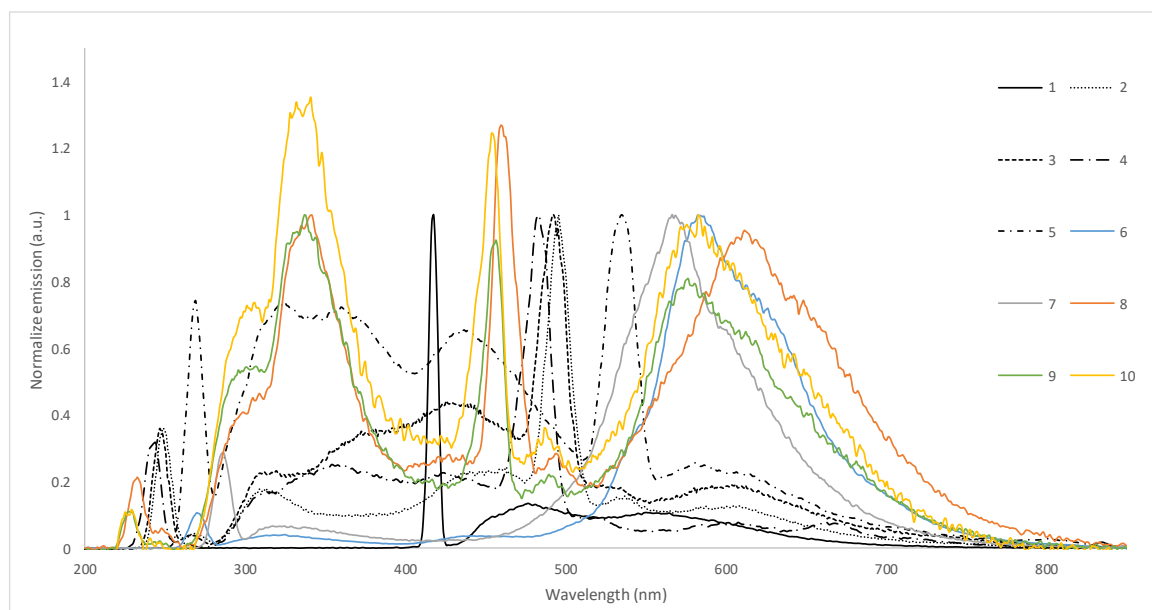


Figure 3. Normalized fluorescence spectra of anthraquinones 1-10

Table 2. Excitation wavelengths, emission bands, and Stokes shift of anthraquinones 6-10

Compound	Excitation (nm)	Emission maxima			Emission maxima in visible region		
		Emission	Intensity	Stokes Shift (nm)	Emission (nm)	Intensity	Stokes Shift (nm)
6	269	583	641.40	316	583	641.40	316
7	285	567	721.61	282	567	721.61	282
8	230	342	112.79	112	612	107.36	382
9	223	338	242.61	115	577	196.34	354
10	222	341	176.68	119	583	130.48	361

substitution at the very low field region in the ^1H -NMR spectra indicated the presence of internal hydrogen bonding between the proton of the hydroxyl substitution with the proximate heteroatom such as between 1-OH with C-9 carbonyl. The ^{13}C -NMR spectra were dominated by the sp^2 -type methine and quaternary of carbon signals associated with the anthraquinone core structure. The presence of the sp^3 -type ^{13}C -NMR signal is often due to the substitution group such as OMe and Me. Another characteristic of the anthraquinone ^{13}C -NMR spectra was the presence of two carbonyl signals at δ_{C} 180-190.

DISCUSSIONS

Substituent groups play a major role in the transmission of the absorption and emission bands in anthraquinone. The nature of the substituent group (electron donating or withdrawing) coupled with the substitution position are the dominating factors resulting in band transmission to red- or blue-shift in the spectra. The ability to form hydrogen bonding and other intermolecular interactions affects the photochemical characteristic of anthraquinone significantly [12,14,18]. The presence of a strong electron-donating substituent can induce charge-

transfer from the substituent to the anthraquinone conjugated system and results in a red-shift band transition in the visible region. In anthraquinones **6-10**, only electron-donating substitution groups were present and hence accounted for the observed red-shift transition as a result of the factors mentioned above.

The position of the OH substitution group was critical as it was able to extend the ring system of anthraquinone through the intramolecular hydrogen bonding between the OH substitution with the proximate oxygen atom (Fig. 4). The ring system extension resulted in the red-shift band displacement in both the absorption and emission spectra, especially in the visible region. The observations of the OH signals at higher field regions in the ^1H -NMR spectra exemplified by $\delta_{1\text{-OH}}13.12$ for **6**, $\delta_{1\text{-OH}}14.81$ and $\delta_{3\text{-OH}}12.63$ for **7**, $\delta_{1\text{-OH}}13.03$ for **9**, and $\delta_{2\text{-OH}}13.02$ for **10** suggested that these OHs formed intramolecular hydrogen bondings with the proximate oxygen atom, and hence supporting the presence of the additional ring. The intermolecular hydrogen bondings also played an important role in lengthening the system conjugation by forming the solvent-compound complex exemplified in **10** (Fig. 5) [12,14], and contributed to the red-shift band displacement. The

persistence association of complexes due to intermolecular hydrogen bondings and other interactions resulted in the broadening of the bands in the visible region [14].

Anthraquinone **8** showed the longest emission band and Stokes shift at 612 and 382 nm, respectively. The observation of the largest red-shift band displacement in the visible region was due to the presence of multiple electron-donating substituents in the structure of **8**, i.e., three hydroxyls and one methyl, favorably extending the system conjugation. The large Stokes shift was a result of the fast relaxation from the initial to emission state via intramolecular energy transfer.

On the other hand, anthraquinone **7** showed the shortest emission band and Stokes shift in the visible region, at 567 and 282 nm, respectively. The structure of anthraquinone **7** possessed hydroxyl substituents at C-1 and C-3, and a methoxy group at C-2. These electron-donating substituents were able to

form two additional rings through hydrogen bonding (Fig. 4). The blue-shift bands transition displayed by the emission spectra of **7** could be attributed to steric hindrance due to the proximate presence of substituents at C-1, C-2, and C-3. The steric hindrance caused the spacial configuration of anthraquinone **7** to adopt a less planar structure, decreasing the electron donating efficiency of the substituent and leading to disturbance in the system hyper-conjugation, and finally resulted in blue-shift transition [14]. Lastly, anthraquinones **6-10** did not exhibit phosphorescence properties in the present investigation.

CONCLUSION

The present report focuses on characterizing the photophysical properties of natural anthraquinone. The presence of the electron-donating substituent in the anthraquinone structure resulted in the general red-shift transition in both absorption and emission spectra. The red-shift transition could be further strengthened by strategic placement of the substitution

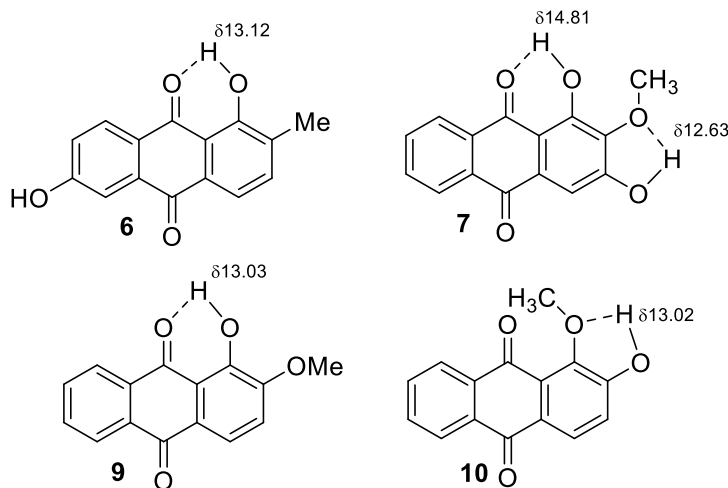


Figure 4. Intramolecular hydrogen bonding extended the anthraquinone ring system

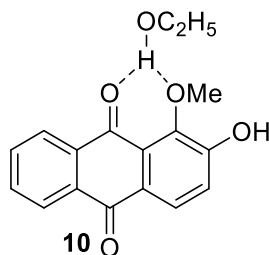


Figure 5. Ethanol-anthraquinone complex through intermolecular hydrogen bondings

group, which allowed formation of an additional ring through intramolecular hydrogen bonding, and hence extending the system conjugation. The formation of the additional quasi-aromatic was also supported by the observed $^1\text{H-NMR}$ data. The possibility to tune the absorption/emission band to red- or blue-region is an excellent tool to manipulate the character and property of these compounds as dyes and sensors. It is interesting to note that anthraquinone **6** and **7** displayed strong emission bands in the visible region only, indicating the highly selective characteristic of these compounds, which is a desirable trait in the chemical sensor development research.

ACKNOWLEDGEMENT

This work was supported by University Malaya Research Grant (RP002A-13Bio and RP002B-13Bio), and University of Malaya SATU research grant (ST004-2018).

REFERENCES

- Harris, R. M. (1999) A Primer on Colorful Additives, in *Coloring Technology for Plastics*, eds. R.M. Harris, William Andrew Publishing: Norwich, New York.
- Puerner, F., Schieven, J. and Hilt, G. (2013) Synthesis of fluorenone and anthraquinone derivatives from aryl- and aroyl-substituted propiolates, *Org. Lett.*, **18**, 4888–4891.
- Seidel, N., Hahn, T., Liebing, S., Seichter, W., Kortus, J. and Weber, E. (2013) Synthesis and properties of new 9,10-anthraquinone derived compounds for molecular electronics, *New J. Chem.*, **37**, 601–610.
- Wcislo, A., Niedziałkowski, P., Wnuk, E., Zarzeczanska, D. and Ossowski, T. (2013) Influence of different amino substituents in position 1 and 4 on spectroscopic and acid base properties of 9, 10-anthraquinone moiety, *Spectrochim Acta Mol. Biomol. Spectroscopy*, **108**, 82–88.
- Weisstuch, J. and Testa, A. C. (1970) Fluorescence study of 2-(*N,N*-Dimethylamino) pyridine and related molecules, *J. Phys. Chem.*, **74**, 2299–2302.
- Caro, Y., Petit, T., Grondin, I., Fouillaud, M. and Dufossé, L. (2017) Hydroxyanthraquinone dyes from plants, in *Symposium on natural colorants “Plants, Ecology and Colours”* May 2017, Antananarivo, Madagascar, hal-01518543.
- Duval, R. and Duplais, C. (2017) Fluorescent natural products as probes and tracers in biology, *Nat. Prod. Rep.*, **34**, 161–193.
- Zhao, Y., Xu, Z. and Lin, T. (2016) Barrier textiles for protection against microbial, in *Antimicrobial Textiles*, eds. S. Gang, Woodhead Publishing: United Kingdom, 225–245.
- Zhuo, J. (2016) Photoactive chemicals for antimicrobial textiles, in *Antimicrobial Textiles*, eds. S. Gang, Woodhead Publishing: United Kingdom, 197–223.
- Kamiya, K., Hamabe, W., Tokuyama, S., Hirano, K., Satake, T., Kumamoto-Yonezawa, Y., Yoshida, H. and Mizushima, Y. (2010) Inhibitory effect of anthraquinones isolated from the Noni (*Morinda citrifolia*) root on animal A-, B- and Y-families of DNA polymerases and human cancer cell proliferation, *Food Chemistry*, **118**(3), 725–730.
- Ngo, J. S. K., Ong, W. K., Ahmad, F. B. and Bujang, K. B. (2013) A study of soluble-powdered natural dyes, *Research Journal of Textile and Apparel*, **17**(1), 104–112.
- Adnan, N. E., Mohd Nasuha, N. A., Abdullah, Z., Tajuddin, H. A. and Choo, Y. M. (2018) Isolation and Photophysical Properties of Di- and Tri-substituted Natural Anthraquinones from Malaysian *Morinda citrifolia*, *Sains Malaysiana*, **47**(5), 903–906.
- Anouar, E. L., Osman, C. P., Weber, J. F. F. and Ismail, N. H. (2014) UV/Visible spectra of a series of natural and synthesised anthraquinones: experimental and quantum chemical approaches, *SpringerPlus*, **3**, 233.
- Diaz, A. N. (1990) Absorption and emission spectroscopy and photochemistry of 1,10-anthraquinone derivatives: a review, *J. Photochem Photobio A: Chemistry*, **53**, 141–167.
- Diaz, A. N. (1991) Analytical applications of 1,10-anthraquinones: A review, *Talanta*, **38**, 571–588.
- Allen, N. S., Pullen, G., Shah, M., Edge, M., Holdsworth, D., Weddell, I. and Catalina, F. (1995) Photochemistry and photoinitiator properties of 2-substituted anthraquinones 1. Absorption and luminescence characteristics, *J. Photochem Photobio A: Chemistry*, **91**, 73–79.
- Peters, R. H. and Sumner, H. H. (1953) Spectra of anthraquinone derivatives, *J. Chem. Soc.*, 2101–2110.
- Flom, S. R. and Barbara P. F. (1985) Proton transfer and hydrogen bonding in the internal conversion of S1 anthraquinones, *J. Phys. Chem.*, **89**, 4489–4494.